

Molecular Dynamics Study of Ice Crystallite Melting

Thomas A. Weber* and Frank H. Stillinger

Bell Laboratories, Murray Hill, New Jersey 07974 (Received: August 23, 1982; In Final Form: November 23, 1982)

The method of molecular dynamics computer simulation has been used to examine the melting process for a 250-molecule ice Ih crystallite. The ST2 potential was used to represent interactions, and the equations of motion were integrated without spatial cutoffs on those interactions. Melting was observed to begin at the crystallite surface and to proceed inward, eventually converting the entire structure to a labile, amorphous droplet. The results suggest that the melting point for the classical ST2 model is about 300 K. Stereoscopic pictures are presented of cluster configurations encountered during the melting process.

I. Introduction

Computer simulation has produced valuable insights into the molecular nature of water in both its liquid¹⁻⁵ and solid^{6,7} forms. However, this technique thus far has had no application to the study of phase transitions in water, in spite of the fact that it has proved to be a potent tool for the study of transitions in other substances.⁸ In this paper we report some molecular dynamics simulation results that were created in an attempt to understand more deeply the melting and freezing of water under ordinary pressures.

As explained in section II, our calculations have employed a conventional and well-documented potential for the water interactions, the "ST2" potential.⁹ But in several other respects the present project has broken with simulation tradition. In the first place, we do *not* use periodic boundary conditions but instead examine an isolated cluster of 250 molecules so that the nature and role of free surfaces in the melting process can be properly evaluated. In the second place, we invoke *no* cutoff on molecular interactions but face up to the difficult necessity of including all pair potentials regardless of molecular separation. From the outset it was our belief that these features were mandatory in order to maximize the scientific significance of the project.

Section III presents our results. They demonstrate vividly that the melting process begins at the cluster surface and moves inward eventually to consume the entire hexagonal ice crystallite with which the simulation began. This investigation establishes that the melting point of the purely classical ST2 model for water is close to 300 K.

The present study raises several interesting prospects for future research which we discuss briefly in section IV.

II. Crystallite Dynamics

We decided at the beginning of this study to examine the properties of a relatively large cluster with free surfaces. Consequently, the potential energy contains two types of terms, namely those that describe interactions between

pairs of water molecules and those that serve as "wall" interactions to keep the system bounded in size and in location.

The ST2 potential was employed to represent molecular pair interactions.⁹ This model potential treats water molecules as rigid asymmetric rotors, accounts for hydrogen bonding, and appears to be successful in producing the characteristic thermodynamic anomalies exhibited by liquid water in bulk.⁹

The wall potential has the following form

$$U(r_i) = \cosh(ar_i)/\cosh(ar_0) \quad (2.1)$$

Here r_i is the distance in Å from the origin to the center-of-mass of molecule i

$$a = 2 \text{ \AA}^{-1} \quad r_0 = 20 \text{ \AA} \quad (2.2)$$

and U as shown has units kcal/mol. Since U monotonically increases with r_i it constitutes a nonwetting boundary. For the number of molecules used in our calculation (250) the wall potential typically acts only very weakly on molecules, even those at the cluster periphery. The effect is to keep the cluster centered near the origin and to reflect back into the cluster those few molecules which might evaporate.

It was first necessary to construct a cluster configuration corresponding to a compact piece of hexagonal ice. For this purpose an extended hexagonal ice lattice was formed by periodic replication of an eight-molecule unit cell. This unit cell was selected to have no net dipole (so the resulting extended lattice would be unpolarized), and to lead to perfect hydrogen bonding to its periodic images in the manner decreed by the "ice rules". The unit cell dimensions are (7.93545, 4.49073, 7.33333) Å, and its eight molecules have configurations specified in Table I.

A spherical region containing exactly 250 molecules was excised from within the extended ice Ih lattice. This operation leaves molecules in the resulting cluster at positions of unbalanced force and torque, particularly those at the surface. Therefore a relaxation process was carried out to bring the cluster to a potential energy minimum (vanishing forces and torques on all molecules) by solving suitably damped equations of motion. This relaxation causes some surface reconstruction to occur. Figure 1a shows a stereoscopic view of the fully relaxed 0 K ice crystallite viewed in the basal plane. Figure 2a shows the same configuration viewed along the hexagonal c axis.

It should be stressed that the existence of this fully relaxed cluster demonstrates the ability of the ST2 potential to yield stable hexagonal ice. We find that the average distance between nearest-neighbor oxygen atoms in the interior of this crystallite is 2.774 Å, which compares

- (1) A. Rahman and F. H. Stillinger, *J. Chem. Phys.*, **55**, 3449 (1971).
- (2) A. Rahman and F. H. Stillinger, *J. Am. Chem. Soc.*, **95**, 7943 (1973).
- (3) S. Swaminathan and D. L. Beveridge, *J. Am. Chem. Soc.*, **99**, 8392 (1977).
- (4) W. L. Jorgensen, *Chem. Phys. Lett.*, **70**, 326 (1980).
- (5) D. C. Rapaport and H. A. Scheraga, *Chem. Phys. Lett.*, **78**, 491 (1981).
- (6) A. Rahman and F. H. Stillinger, *J. Chem. Phys.*, **57**, 4009 (1972).
- (7) R. M. J. Cotterill, J. W. Martin, O. V. Nielsen, and O. B. Pedersen in "Physics and Chemistry of Ice", E. Whalley, S. J. Jones, and L. W. Gold, Ed., Royal Society of Canada, Ottawa, 1973, pp 23-7.
- (8) M. Parrinello and A. Rahman, *Phys. Rev. Lett.*, **45**, 1196 (1980).
- (9) F. H. Stillinger and A. Rahman, *J. Chem. Phys.*, **60**, 1545 (1974).

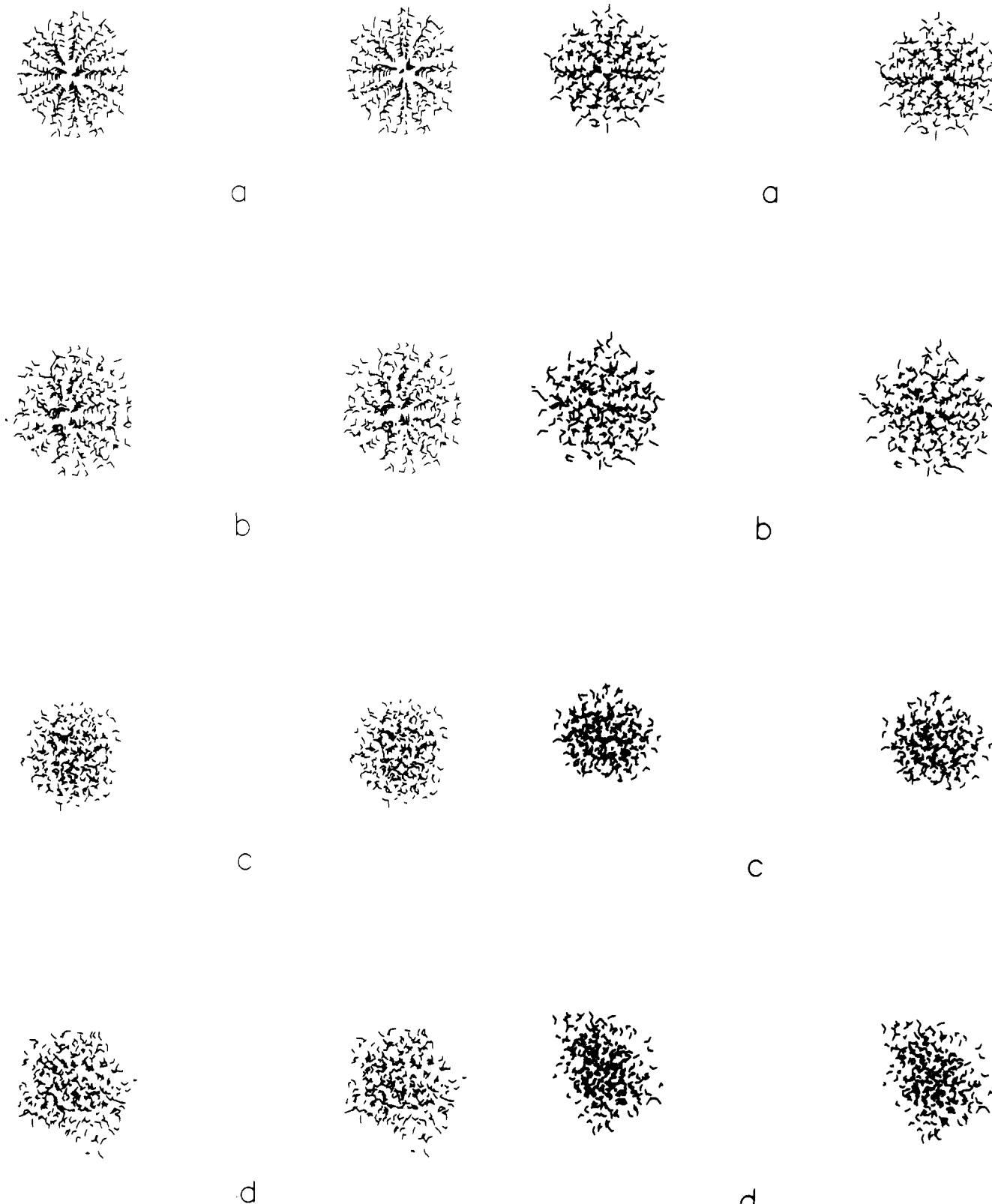


Figure 1. Stereoscopic pictures of cluster configurations, viewed in a direction parallel to the basal plane of the starting crystallite: (a) 0 K, (b) 249 K, (c) 300 K, (d) 356 K.

favorably with the value 2.75 Å that has been measured for real ice.¹⁰

We have used Evans' method of quaternion variables¹¹ to solve numerically the dynamical equations for the 250

Figure 2. Stereoscopic pictures of cluster configurations, viewed in a direction aligned with the *c* axis of the starting crystallite: (a) 0 K, (b) 249 K, (c) 300 K, (d) 356 K.

molecules. This procedure eliminates singularities that arise in a more straightforward solution of the coupled Euler-Lagrange equations. We find that the time increment 4×10^{-4} ps can be used in the numerical analysis while maintaining an adequate level of energy invariance. No cutoffs were applied to the pair potential; the full ST2 interaction operated between all pairs of molecules at each integration step. Each picosecond of "real" time for the

(10) N. H. Fletcher, "The Chemical Physics of Ice", Cambridge University Press, London, 1970, p 26.

(11) D. J. Evans, *Mol. Phys.*, **34**, 317 (1977).

TABLE I: Unit Cell Configuration for Hexagonal Ice^a

molecule	<i>x</i>	<i>y</i>	<i>z</i>	ξ^b	η	ρ	χ
1	2.592 72	2.245 37	0.916 67	$\alpha_1\sqrt{3}$	α_1	$-\alpha_2$	$\alpha_2\sqrt{3}$
2	3.889 09	0	0	$-\alpha_2$	α_3	α_4	α_1
3	6.639 09	0	0.916 67	$\alpha_2\sqrt{2}$	$\alpha_2\sqrt{2}$	$\alpha_1\sqrt{2}$	$-\alpha_1\sqrt{2}$
4	7.935 45	2.245 37	0	0	$2\alpha_2$	$2\alpha_1$	0
5	2.592 72	2.245 37	3.666 67	α_2	$-\alpha_3$	α_4	α_1
6	3.889 09	0	4.583 33	$\alpha_1\sqrt{3}$	α_1	α_2	$\alpha_2\sqrt{3}$
7	6.639 09	0	3.666 67	0	$2\alpha_2$	$2\alpha_1$	0
8	7.935 45	2.245 37	4.583 33	$-\alpha_2\sqrt{2}$	$-\alpha_2\sqrt{2}$	$\alpha_1\sqrt{2}$	$-\alpha_1\sqrt{2}$

^a Cartesian coordinates *x*, *y*, *z* specify center of mass positions in Å. Unit cell dimensions are $l_x = 7.93545$ Å, $l_y = 4.49073$ Å, $l_z = 7.33333$ Å. Molecule orientations are specified by quaternion variables ξ , η , ρ , χ ; for their definition in terms of Euler angles see Evans, ref 11. ^b $\alpha_1 = 1/2[1/2(1 - 3^{-1/2})]^{1/2}$, $\alpha_2 = 1/2[1/2(1 + 3^{-1/2})]^{1/2}$, $\alpha_3 = 1/2[1/2(3 - 5 \times 3^{-1/2})]^{1/2}$, $\alpha_4 = 1/2[1/2(3 + 5 \times 3^{-1/2})]^{1/2}$.

TABLE II: Cluster Properties^a

<i>E</i>	<i>t</i>	<i>T</i>	$\langle\mu^2\rangle^{1/2}$	<i>I</i> ₁	<i>I</i> ₂	<i>I</i> ₃	H bonds
-12.333 018	0	0.0	15.30	4.419	4.655	4.908	439.0
-10.400 842	1	149.8	6.02	4.508	4.698	5.038	390.0
-9.804 248	1	196.0	7.17	4.469	4.738	5.016	372.5
-8.958 126	2	248.5	16.94	4.493	4.767	5.087	339.4
-8.549 740	2	267.9	22.54	4.504	4.794	5.139	320.6
-8.237 514	2	281.8	16.58	4.649	4.884	5.146	309.6
-7.990 903	2	287.4	19.30	4.723	4.904	5.228	295.8
-7.741 423	4	296.5	17.15	4.778	5.257	5.715	278.6
-7.494 010	4	300.0	17.21	4.694	5.872	6.304	262.5
-7.264 999	4	303.4	20.21	4.830	6.488	7.186	249.3
-7.005 871	2	309.3	14.62	4.921	6.933	7.865	233.6
-6.756 986	2	314.8	18.46	5.191	7.083	7.925	222.2
-6.274 848	2	334.1	22.52	5.564	7.298	7.690	209.0
-5.750 500	2	356.0	18.06	5.645	6.918	7.264	178.4
-7.262 269	2	288.4	16.48	4.750	5.745	6.250	240.8

^a *T*, K; μ , D; $10^{35}I$, g cm²; *t*, ps; *E*, kcal/mol.

system's motion consumed about 200 min of computing time on a CRAY 1.

Starting with small random translational and rotational momenta assigned to the molecules, we heated the system in stages by homogeneous momentum scaling. At each temperature of interest a period of equilibration was allowed to pass (typically 0.2 ps) before dynamical averaging was performed. This latter spanned periods of either 1, 2, or 4 ps depending on whether or not substantial melting was underway.

In addition to the sequence of cluster states generated by successive heatings of the initial ice configuration, a single additional state was also examined. This last state was created from an initial arrangement of water molecules with random positions and orientations. It was cooled and reheated several times before being equilibrated in an essentially liquidlike state.

III. Cluster Melting

Table II lists some of the calculated cluster properties. The first 14 states shown represent the sequential heating of the hexagonal ice structure. The last state listed is the one created from random initial conditions for the 250 molecules. In addition to the energy of the given state, Table II provides the length of the time interval used for averaging, the mean temperature (from translational and rotational kinetic energy), the rms cluster dipole moment, and the three mean inertial moments.

The last column in Table II shows the average number of hydrogen bonds exhibited by each state. For present purposes we have defined hydrogen bonds to be equivalent to the existence of ST2 pair interactions falling below the "cutoff" value

$$V_{\text{HB}} = -4.0 \text{ kcal/mol} \quad (3.1)$$

This kind of potential energy criterion for hydrogen

bonding has been invoked before.^{2,12} The specific choice for V_{HB} is rather stringent but nevertheless has the effect of identifying four hydrogen bonds to each water molecule within the deep interior of the 0 K crystallite.

Stereoscopic pictures have been produced of the final molecular configurations for each cluster state. Some of these are shown in Figures 1 and 2. Those presented in Figure 1 all are views along a spatial direction that was parallel to the basal plane of the starting crystallite; Figure 2 presents a *c*-axis view of the same set of configurations.

The fully relaxed hexagonal ice crystallite at 0 K is shown in Figures 1a and 2a. The periodic structure of the extended ice lattice is obviously present within the interior of this spherical cluster. It is also obvious from these pictures that water molecules at the surface of the crystallite have moved substantially away from the starting lattice positions. We have found in particular that hexagons of hydrogen bonds normally present in the lattice interior can occasionally be replaced by pentagonal arrangements, as a result of surface reconstruction (one is visible at the back of Figure 2a).

Figure 3 shows the energies of the 15 states plotted against absolute temperature. At low temperature it appears that most of the energy increase with rising temperature can be attributed to harmonic motion (heat capacity per molecule $6k_B$). However, the behavior becomes increasingly anharmonic as revealed by a growing slope. The slope achieves a maximum at approximately 300 K, which we take to be a rough indication of the melting point for the ST2 model.

The single amorphous state produced from random initial conditions has been indicated by a square in Figure 3. This state and the two highest temperature states from

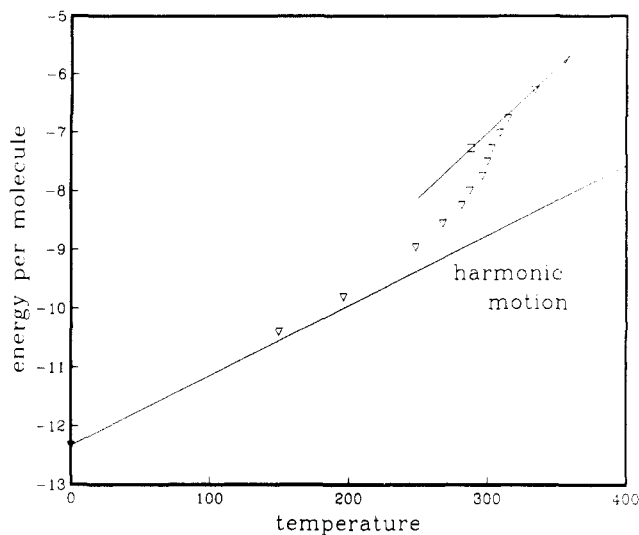


Figure 3. Mean energy per molecule (in kcal/mol) for the 250 molecule cluster. The 14 triangles are results from sequential heating of the hexagonal ice crystallite. The point indicated by a square is a supercooled liquid droplet formed from random initial conditions (see text).

the crystallite heating (triangles) have been connected by a least-squares line. The slope of this line is substantially larger than that for harmonic motion and is found to correspond to a heat capacity per molecule of $11.16k_B$. This is evidently the thermodynamic behavior appropriate for a tiny liquid droplet comprising 250 molecules, at least in the classical ST2 model approximation.

Careful examination of the stereopictures in Figures 1 and 2 show that the melting process for the ice crystallite begins at its surface and proceeds inward. Already at 249 K (Figures 1b and 2b) the weakly bonded molecules show considerably greater disordering than those within the inner core. Figures 1c and 2c show the crystallite at its "melting point", with a considerable liquidlike mantle surrounding a still-icy core. The central icelike core has entirely vanished in the 356 K state (Figures 1d and 2d).

In order to provide quantitative documentation for the radially-inward melting observation, we have calculated hydrogen bond distributions separately for cluster core and mantle regions. Water molecules comprising the core are defined to be those lying within 9.0 Å of the origin; typically this would include about 90 molecules out of the 250. The mantle is the remainder outside this core. The molecules in these two sets were classified according to the numbers of hydrogen bonds in which they were engaged, using data taken at the end of each 0.4 ps during each state's averaging interval. Figure 4 displays core and mantle histograms for occurrence probabilities of molecules with 0, 1, 2, 3, or 4 hydrogen bonds according to criterion (3.1). While it is possible in principle for five-bonded molecules to exist they were only rarely encountered in our calculation and so have been disregarded for the purposes of the figure.

Notice that, while the core is entirely four bonded at 0 K, the mantle in the same state is imperfectly bonded even after surface reconstruction has taken place. As temperature rises both subset distributions move to lower average numbers of hydrogen bonds, but the core region continues to maintain a higher average bonding than the mantle.

Figure 5 provides a comparison of the partially melted crystallite at 287.4 K and the amorphous droplet (from random initial conditions) at the nearly identical temperature 288.4 K. For this pair of states the mantle distributions are relatively similar, while the core distributions differ significantly.

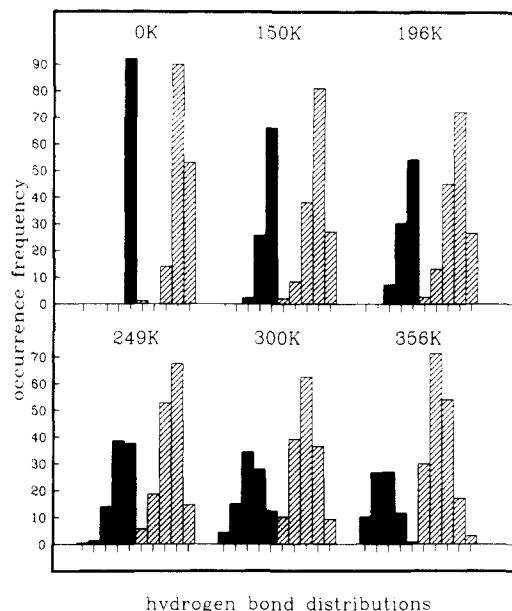


Figure 4. Occurrence frequencies for hydrogen bond numbers in cluster core (solid bars) and mantle (hatched bars). For each temperature the ten positions from left to right refer to 0-, 1-, 2-, 3-, and 4-bonded core molecules, 0-, 1-, 2-, 3-, and 4-bonded mantle molecules.

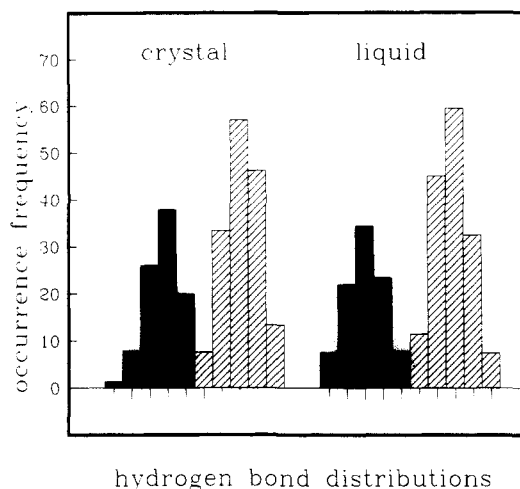


Figure 5. Hydrogen-bond-number occurrence frequencies for the largely unmelted crystallite at 287.4 K (at left) and a supercooled liquid droplet at 288.4 K (at right).

IV. Discussion

The calculations reported here support the hypothesis originating with Faraday that ice not too far below its melting point is covered by a liquidlike layer¹³. Qualitatively this is easy to understand, for the strongly directional tetrad of hydrogen bonds that firmly holds an interior molecule in place in the ice lattice is severely disrupted at the surface. Even at 0 K surface restructuring is expected and was observed in our calculations. Under the circumstances it is not surprising that well below the bulk crystal melting point surface region molecules should exhibit substantial lateral mobility. We believe that one potentially significant extension of our simulation would be the direct study of rate of surface-molecule rotational and translational diffusion as a function of temperature, since this evidently bears on crystal growth phenomena.

It would also be interesting and feasible to study the melting of defective ice. This would simply require se-

lection of an alternative starting configuration, say an ice crystallite with an impurity molecule or a buried vacancy. With this condition melting might begin at the defect as well as at the free surface.

The fact that the crystallite does not melt at a sharply defined temperature is due in part to the small system size, and in part to the rapid rate of temperature rise. With respect to the *position* of the identified melting temperature (300 K, the inflection point in Figure 3), the first of these features tends strongly to mitigate the second. Since calculations of the hexagonal ice binding energy indicate that the ST2 interaction is roughly 10% too strong,¹⁴ it is consistent that the observed ST2 "melting point" is about 10% too high.

By reducing the parameter r_0 in the wall potential U , eq 2.1, it should be possible to study the melting of ice

under pressure. It will eventually be instructive to see if the ST2 potential (as well as others that have been used in water simulations) can produce the phenomenon of lowered melting points at elevated pressure observed for real ice Ih.

We have not attempted to refreeze the melted clusters, since spontaneous nucleation of ice from the liquid is expected to have negligible probability under the conditions used in our calculations. Stepwise cooling of the 356 K liquid droplet is expected only to trace out the upper straight line in Figure 3, for instance, and to produce supercooled liquid water as represented by the square in Figure 3. However, the attractive option exists to cool one of the partially melted states, the icy core of which might act as a nucleus on which the melted mantle could epitaxially grow.

(14) M. D. Morse and S. A. Rice, *J. Chem. Phys.*, 76, 650 (1982).

Registry No. Water, 7732-18-5.

Ice under Pressure: Transition to Symmetrical Hydrogen Bonds

Frank H. Stillinger* and Kenneth S. Schweizer

Bell Laboratories, Murray Hill, New Jersey 07974 (Received: August 23, 1982)

We have examined at a rudimentary level the quantum-mechanical many-body problem for coupled proton motions along hydrogen bonds in compressed ices. Four cases are considered: ice Ic, ices VII and VIII, and the hypothetical planar "square ice". Soft mode calculations were carried out for each to help identify patterns of long-range proton order that contribute to the ground state. With a two-level description of each hydrogen bond, and the Hartree approximation, a phase transition in the ground state is predicted to occur when the oxygen neighbor spacing has been reduced sufficiently. This transition can be viewed as an "ionization catastrophe", and in fact such is expected to occur at all temperatures in the phase diagram of water at which ices VII and VIII experimentally are encountered.

1. Introduction

An interesting structural correlation has been known for many years concerning hydrogen bonds connecting oxygen atoms in crystals at ordinary pressures.^{1,2} Specifically this correlation shows that covalent O-H bond lengths stretch as r_{OO} , the distance between hydrogen-bonded oxygens, decreases. In particular the data indicate that when the participating oxygens are as close, or closer, than about 2.4 Å the hydrogen should be found at the midpoint position. Indeed such symmetrical hydrogen bonds are observed in crystals at 1 atm, though only in ionic groupings (solvated H^+ or OH^-).

These observations suggest that if pressure were applied to substances containing hydrogen-bonded oxygens so as to vary the relevant oxygen separation, the same correlation should obtain. In particular if the substance were ice, then application of pressure sufficient to reduce the neighbor distance to about 2.4 Å ought to have the effect of converting the asymmetric hydrogen bonds to symmetric form. The pressures required for this transformation are expected to be sufficiently high that it is the ice VII and ice VIII regions of the H_2O phase diagram that would

require exploration. Walrafen et al. have in fact recently examined ice VII to about 30 GPa (where $r_{OO} \approx 2.5$ Å) and have observed a remarkable drop in the frequency of O-H stretching vibrations,³ which likely is symptomatic of substantial increase in the equilibrium O-H bond length toward a midpoint position.

The possibility of a pressure-induced transition in ice to a new form with symmetrical hydrogen bonds has been theoretically considered before. Holzapfel⁴ has examined the linear motion of a single proton between two neighboring oxygens, where that proton was subject to the presence of a pair of equivalent Morse potentials. He finds that the critical bond length

$$r_{OO} = 2.41 \text{ \AA} \quad (1.1)$$

separates the two regimes of proton potential characterized respectively by a single minimum at the bond midpoint, and by a pair of equivalent minima displaced from the midpoint.

By treating the proton classically in Holzapfel's one-particle model (i.e., searching for the potential minimum at each r_{OO}), it is straightforward to show that the crystal energy will exhibit a singularity in r_{OO} (or pressure) at the critical lattice spacing (1.1). By itself this might seem to

(1) G. C. Pimentel and A. L. McClellan, "The Hydrogen Bond", Freeman, San Francisco, 1960, p 259.

(2) J.-O. Lundgren and I. Olovsson, "The Hydrated Proton in Solids", in "The Hydrogen Bond. II. Structure and Spectroscopy", P. Schuster, G. Zundel, and C. Sandorfy, Ed.; North Holland, New York, 1976, p 497.

(3) G. E. Walrafen, M. Abebe, F. A. Mauer, S. Block, G. J. Piermarini, and R. Munro, *J. Chem. Phys.*, 77, 2166 (1982).

(4) W. B. Holzapfel, *J. Chem. Soc.*, 56, 712 (1972).